Heat and Mass Transfer in Power-Law Nanofluids Over a Nonisothermal Stretching Wall With Convective Boundary Condition

Waqar A. Khan[1]
Department of Engineering Sciences,
PN Engineering College,
National University of Sciences and Technology,
Karachi 75350, Pakistan
e-mail: wkhan_2000@yahoo.com

Rama Subba Reddy Gorla
Department of Mechanical Engineering,
Cleveland State University,
Cleveland, OH 44114

A boundary layer analysis that has been presented for the heat and mass transfer in power-law nanofluids over a stretching surface with convective boundary condition are investigated numerically. The surface nanoparticle concentration is kept constant. A power-law model is used for non-Newtonian fluids, whereas Brownian motion and thermophoresis effects are incorporated in the nanofluid model. A similarity transformation is used to reduce mass, momentum, thermal energy, and nanoparticles concentration equations into nonlinear ordinary differential equations which are solved numerically by using a finite difference method. The effects of nanofluid parameters, suction/injection, and convective parameters and generalized Pr and Le numbers on dimensionless functions, skin friction, local Nusselt, and Sherwood numbers are shown graphically. The quantitative comparison of skin friction and heat transfer rates with the published results for special cases is shown in tabular form and is found in good agreement. [DOI: 10.1115/1.4007138]

Keywords: power-law nanofluids, convective boundary, power-law model, Brownian motion, thermophoresis, skin friction, local Nusselt and Sherwood numbers, stretching surface

1 Introduction

The flow of generalized Newtonian fluids over a stretching surface can be found in many engineering processes with applications in industries, such as extrusion, the hot rolling, wire drawing, melt-spinning, glass-fiber production, manufacture of plastic and rubber sheets, cooling of a large metallic plate in a bath, etc. The boundary layer flow of a generalized Newtonian fluid caused by the stretching of an elastic flat sheet has been studied by a number of researchers and a good amount of literature exists on this problem, e.g., [1–13].

The boundary layer flow of a Newtonian based nanofluid past a stretching sheet is gaining interest in industries due to higher thermal conductivity of nanofluids. A comprehensive survey of convective transport in nanofluids was made by Buongiorno [14]. Recently, Kuznetsov and Nield [15] have examined the influence of nanoparticles on natural convection boundary-layer flow past a vertical plate, using a model in which Brownian motion and thermophoresis are accounted for. Later on, Khan and Pop [16] extended their work for the flow over a stretching surface in a nanofluid. Vajravelu et al. [17] investigated the convective heat transfer in a nanofluid flow over a stretching surface. They focused on Ag–water and Cu–water nanofluids, and investigated the effects of the nanoparticle volume fraction on the flow and heat transfer characteristics under the influence of thermal buoyancy and temperature dependent internal heat generation or absorption. 'Makinde and Aziz [18] studied the boundary layer flow induced in a nanofluid due to a linearly stretching sheet by using a convective heating boundary condition.

The above literature review reveals that in most of the previous investigations, Newtonian fluids were used as base fluids. Non-Newtonian nanofluids (non-Newtonian fluids with dispersed nanoparticles) have been used by only few researchers including Chen et al. [19], Ding et al. [20,21], and Chen et al. [19,22]. More work is needed to investigate the characteristics of nanofluids and the mechanism of the forced convective heat transfer of nanofluids [23]. To the best of our knowledge, there is no study related to heat and mass transfer in power-law nanofluids over a stretching surface with convective boundary condition.

The objective of the present study is to extend the work of Hassanien et al. [13] to analyze the behavior of power-law nanofluids over a stretching surface in a nanofluid with convective boundary condition and uniform surface nanoparticle concentration. A similarity solution is obtained that depends upon different power-law nanofluid parameters, such as the generalized Prandtl and Lewis numbers, a Brownian motion number Nb, a thermophoresis number Nt, and the convective parameter h_c. The dependency of the skin friction, the local Nusselt, and the Sherwood numbers on these parameters is investigated numerically. To the best of our knowledge, the results of this paper are new and they have not been published before.

2 Basic Equations

Consider the steady two-dimensional boundary layer flow of a power-law nanofluid past a stretching surface with the linear velocity $u_w(x) = Bx$, where B is a constant and x is the coordinate measured along the stretching surface. The surface is heated by flowing fluid at a temperature T_f with variable heat transfer coefficient $h(x) = A(1-x)^{-n/(n+1)}$, where A is the constant and n is the power-law index. The flow model and coordinate system are shown in Fig. 1. The flow takes place at $y \geq 0$, where y is the coordinate measured normal to the stretching surface. A steady

[1]Corresponding author.

Contributed by the Heat Transfer Division of ASME for publication in the JOURNAL OF HEAT TRANSFER. Manuscript received January 16, 2012; final manuscript received June 26, 2012; published online September 26, 2012. Assoc. Editor: Oronzio Manca.

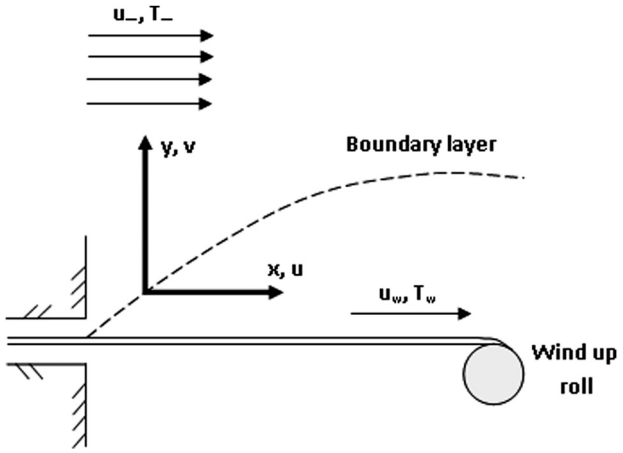

Fig. 1 Flow model and coordinate system

uniform stress leading to equal and opposite forces is applied along the x-axis so that the sheet is stretched keeping to origin fixed. Robin boundary condition is applied at the stretching surface. It is assumed that at the stretching surface, the nanoparticle fraction C take constant value C_w, respectively. The ambient values of temperature and nanoparticle fraction are denoted by T_∞ and C_∞, respectively as $y \to \infty$. The power-law model is used for the non-Newtonian fluid, according to which the relationship between the shear stress and the strain rate is given as follows:

$$\tau_{xy} = \mu \left|\frac{\partial u}{\partial y}\right|^{n-1} \frac{\partial u}{\partial y} \tag{1}$$

When $n = 1$, Eq. (1) represents a Newtonian fluid with dynamic coefficient of viscosity μ and when $n \neq 1$, Eq. (1) represent dilatant or shear-thickening ($n > 1$) and a pseudoplastic or shear-thinning ($n < 1$) fluids with μ as the fluid consistency.

Using scale analysis, the governing mass, momentum, thermal energy, and nanoparticles concentration equations for power-law nanofluids can be written in Cartesian coordinates x and y as in Kuznetsov and Nield [15],

$$\frac{\partial u}{\partial x} + \frac{\partial \mathrm{v}}{\partial y} = 0 \tag{2}$$

$$u\frac{\partial u}{\partial x} + \mathrm{v}\frac{\partial u}{\partial y} = \nu \frac{\partial}{\partial y}\left(\frac{\partial u}{\partial y}\right)^n \tag{3}$$

$$u\frac{\partial T}{\partial x} + \mathrm{v}\frac{\partial T}{\partial y} = \alpha\left(\frac{\partial^2 T}{\partial y^2}\right) + \tau\left\{D_B\left(\frac{\partial C}{\partial y}\frac{\partial T}{\partial y}\right) + \left(\frac{D_T}{T_\infty}\right)\left[+\left(\frac{\partial T}{\partial y}\right)^2\right]\right\} \tag{4}$$

$$u\frac{\partial C}{\partial x} + \mathrm{v}\frac{\partial C}{\partial y} = D_B\left(\frac{\partial^2 C}{\partial y^2}\right) + \left(\frac{D_T}{T_\infty}\right)\left(\frac{\partial^2 T}{\partial y^2}\right) \tag{5}$$

subject to the boundary conditions

$$\begin{aligned} &y = 0: \quad u = Bx, \quad \mathrm{v} = \mathrm{v}_w, \quad -k\frac{\partial T}{\partial y} = h(T_f - T), \quad C = C_w \\ &y \to \infty: \quad u \to 0, \quad T \to T_\infty, \quad C \to C_\infty \end{aligned} \tag{6}$$

Here u and v are velocity components along the axes x and y, respectively, p is the fluid pressure, ρ_f is the density of the base fluid, α is the thermal diffusivity, υ is the kinematic viscosity, a is a positive constant, λ is the temperature parameter, D_B is the Brownian diffusion coefficient, D_T is the thermophoretic diffusion coefficient, and $\tau = (\rho c)_p/(\rho c)_f$ with ρ_f is the density of the fluid, c_f is the specific heat of the fluid, and ρ_p is the density of the particles.

Following Hassanien and Gorla [11] and Hassanien et al. [13], we use the following transformations:

$$\begin{aligned} &\eta = \left(\frac{B^{2-n}x^{1-n}}{\nu}\right)^{1/(n+1)} y, \quad \psi = \left(\nu B^{2n-1}x^{2n}\right)^{1/(n+1)} f(\eta), \\ &\theta(\eta) = \frac{T - T_\infty}{T_f - T_\infty}, \quad \phi(\eta) = \frac{C - C_\infty}{C_w - C_\infty} \end{aligned} \tag{7}$$

where ψ is the stream function and is defined as $u = \partial\psi/\partial y$ and $\mathrm{v} = -\partial\psi/\partial x$, with u and v as the horizontal and vertical components of the velocity, given by

$$\begin{aligned} &u = Bxf' \quad \text{and} \\ &\mathrm{v} = -\left(\nu B^{2n-1}x^{n-1}\right)^{1/(n+1)}\left\{\left(\frac{2n}{n+1}\right)\cdot f + \left(\frac{1-n}{n+1}\right)\cdot \eta f'\right\} \end{aligned} \tag{8}$$

Using transformations (7), Eqs. (3)–(5) can be written as

$$nf'''(f'')^{n-1} + \left(\frac{2n}{n+1}\right)ff'' - f'^2 = 0 \tag{9}$$

$$\frac{1}{\mathrm{Pr}}\theta'' + \left(\frac{2n}{n+1}\right)f\theta' + N_b\phi'\theta' + N_t\theta'^2 = 0 \tag{10}$$

$$\frac{\phi''}{\mathrm{Le}} + \left(\frac{2n}{n+1}\right)f\phi' + \frac{\mathrm{Nt}}{\mathrm{Nb}}\cdot\frac{1}{\mathrm{Le}}\cdot\theta'' = 0 \tag{11}$$

subject to the boundary conditions

$$\begin{aligned} &f(0) = R, \quad f'(0) = 1, \quad \theta'(0) = -h_c(1 - \theta(0)), \quad \phi(0) = 1 \\ &f'(\infty) = 0, \quad \theta(\infty) = 0, \quad \phi(\infty) = 0 \end{aligned} \tag{12}$$

where primes denote differentiation with respect to η and the five parameters are defined by

$$R = \frac{n+1}{2n}\left[\nu B^{2n-1}x^{2n-1}\right]^{-(1/(n+1))}\mathrm{V}_w \tag{13}$$

$$\left.\begin{aligned} \mathrm{Pr} &= \left[\frac{\nu^2 B^{3(n-1)}x^{2(n-1)}}{\alpha^{n+1}}\right]^{1/(n+1)} \\ \mathrm{Le} &= \frac{\nu}{D_B}\left[\frac{B^{3(1-n)}x^{2(1-n)}}{\nu^{1-n}}\right]^{1/(n+1)} \\ \mathrm{Nb} &= \tau D_B(C_w - C_\infty)\left[\frac{B^{3(1-n)}x^{2(1-n)}}{\nu^2}\right]^{1/(n+1)} \\ \mathrm{Nt} &= \frac{\tau D_T(T_w - T_\infty)}{T_\infty}\left[\frac{B^{3(1-n)}x^{2(1-n)}}{\nu^2}\right]^{1/(n+1)} \\ h_c &= \frac{A}{k}\left(\frac{B^{2-n}}{\nu}\right)^{1/(n+1)} \end{aligned}\right\} \tag{14}$$

Here R is the suction/injection parameter which is positive for injection and negative for suction, Prand Le are the generalized Prandtl and Lewis numbers for power-law fluids, Nb and Nt are the generalized Brownian motion and the thermophoresis parameters for power-law nanofluids, respectively, and h_c is the convective parameter. It is important to note that as the convective parameter h_c increases, the heat transfer rates approaches the isothermal case. This statement is also supported by the first thermal boundary condition of (12), which gives $\theta(0) = 1$ as $h_c \to \infty$. It is worth mentioning that for Newtonian fluids ($n = 1$), Eq. (9) satisfies the analytical solution, given by Crane [1]

$$f(\eta) = 1 - e^{-\eta} \tag{15}$$

The dimensionless quantities of practical interest are the friction factor C_f, local Nusselt number Nu_x, and the local Sherwood number Sh_x, which are defined as

$$\begin{aligned} \mathrm{Re}_x^{1/(n+1)} C_f &= 2[f''(0)]^n \\ \mathrm{Re}_x^{-1/(n+1)} \mathrm{Nu} &= -\theta'(0) \\ \mathrm{Re}_x^{-1/(n+1)} \mathrm{Sh} &= -\phi'(0) \end{aligned} \tag{16}$$

where Re_x is the local generalized Reynolds number based on the stretching velocity Bx and is given by

$$\mathrm{Re}_x = \frac{(Bx)^{2-n} x^n}{\nu} \tag{17}$$

Following Kuznetsov and Nield [15], $\mathrm{Re}_x^{-1/(n+1)}\mathrm{Nu}_x$ and $\mathrm{Re}_x^{-1/(n+1)}\mathrm{Sh}_x$ can be referred to as the reduced local Nusselt number *Nur* and reduced local Sherwood number *Shr* for power-law nanofluids, and are represented by $-\theta'(0)$ and $-\phi'(0)$, respectively. It is worth mentioning that Eq. (8) with the boundary conditions (11) has the analytical solution, first obtained by Crane [1].

3 Results and Discussion

The system of transformed governing nonlinear coupled differential equations (9)–(11) with the boundary conditions (12) is solved numerically using an implicit finite-difference scheme with has second-order accuracy with arbitrary spacing. The transformed differential equations and the boundary conditions are first written as a first-order system, which are then converted to a set of finite-difference equations using central differences. Then the nonlinear algebraic equations are linearized by Newton's method and the resulting system of linear equations is then solved by the block tridiagonal elimination technique. A uniform grid of $\Delta\eta = 0.001$ is satisfactory in obtaining sufficient accuracy with an error tolerance less than 10^{-6}. In practice, $\eta = \infty$ must be replaced by an approximation $\eta = \eta_{\max}$, where $\eta_{\max}$ is arbitrary as long as it is chosen large enough so that the solution shows little further change for η larger than $\eta_{\max}$.

Neglecting the effects of Nb and Nt numbers, the results for the dimensionless wall shear stress and the wall heat transfer rate are compared with those obtained by Hassanien et al. [13] for different values of $n, R,$ and h_c in Tables 1 and 2. We notice that the comparison shows good agreement for each generalized Newtonian fluid. Therefore, we are confident that the present results are very accurate. Table 1 shows the dimensionless wall shear stress values for pseudoplastic, Newtonian, and dilatant fluids for suction and injection cases. It is clear that the dimensionless wall

Table 1 Comparison of dimensionless wall shear stress $f''(0)$ for different power-law fluids with Nt = Nb = 10^{-5}

	$n = 0.5$		$n = 1$		$n = 1.5$	
R	Present results	Hassanien et al. [13]	Present results	Hassanien et al. [13]	Present results	Hassanien et al. [13]
−1.5	0.63296	0.633301	0.5	0.500005	0.46014	0.462494
−1	0.759	0.759826	0.61803	0.618042	0.58577	0.586938
−0.5	0.92924	0.931104	0.78078	0.780781	0.75128	0.759664
0	1.16136	1.165235	1	1	0.98001	0.980902
0.5	1.47815	1.485498	1.28078	1.280777	1.22987	1.233108
1	1.90665	1.919345	1.61803	1.618034	1.49989	1.500926
1.5	2.47585	2.495832	2	2	1.77	1.770192

Table 2 Comparison of wall heat transfer $-\theta'(0)$ for different power-law fluids, temperature, and suction/injection parameters with Nt = Nb = 10^{-5} and Pr = 0.72

n	$h_c \rightarrow$ $R \downarrow$	1	100	200	300	400	500	1000	Hassanien et al. [13] $\lambda = 0$
0.5	−1.5	0.06215	0.06655	0.06625	0.06625	0.06626	0.06626	0.06626	0.06643
	−1	0.12121	0.13827	0.13784	0.13787	0.13788	0.13789	0.13791	0.13744
	−0.5	0.19562	0.24321	0.24289	0.24299	0.24304	0.24307	0.24313	0.42229
	0	0.27472	0.37796	0.37806	0.3783	0.37842	0.37849	0.37863	0.37776
	0.5	0.35022	0.53667	0.53754	0.53802	0.53827	0.53841	0.5387	0.53801
	1	0.41798	0.71356	0.71559	0.71644	0.71687	0.71713	0.71764	0.71728
	1.5	0.47689	0.90386	0.9075	0.90887	0.90956	0.90998	0.9108	0.91088
1.0	−1.5	0.04711	0.04907	0.04942	0.04943	0.04943	0.04943	0.04943	0.05044
	−1	0.11409	0.1284	0.1287	0.12873	0.12875	0.12875	0.12877	0.12961
	−0.5	0.2105	0.26585	0.26627	0.26639	0.26645	0.26648	0.26655	0.26701
	0	0.31654	0.46101	0.46208	0.46244	0.46262	0.46272	0.46294	0.46325
	0.5	0.41466	0.70343	0.70591	0.70674	0.70716	0.70741	0.70791	0.6315
	1	0.49736	0.97981	0.98463	0.98625	0.98706	0.98755	0.98853	0.89312
	1.5	0.56428	1.27848	1.28671	1.28947	1.29086	1.29169	1.29336	1.17729
1.5	−1.5	0.0403	0.04131	0.04198	0.04199	0.04199	0.04199	0.04199	0.03489
	−1	0.10604	0.11799	0.11854	0.11857	0.11858	0.11859	0.1186	0.10537
	−0.5	0.20773	0.26136	0.26185	0.26196	0.26202	0.26205	0.26212	0.25277
	0	0.32267	0.47412	0.47526	0.47564	0.47583	0.47594	0.47617	0.48923
	0.5	0.42815	0.78315	0.78592	0.78685	0.78731	0.78759	0.78815	0.79669
	1	0.51495	1.05049	1.05603	1.0579	1.05883	1.05939	1.06051	1.14831
	1.5	0.58344	1.48124	1.49084	1.49408	1.4957	1.49667	1.49863	1.52843

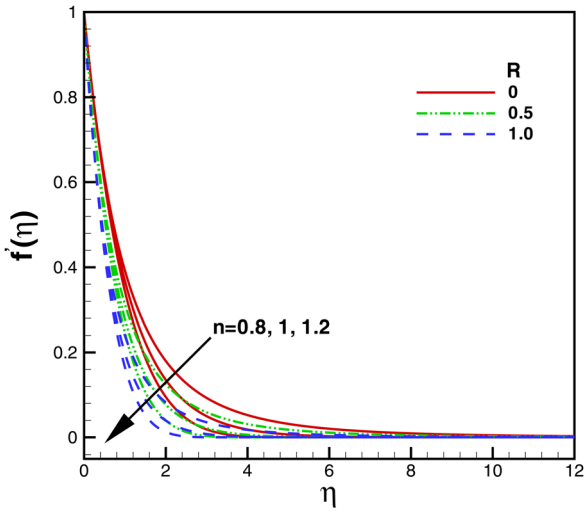

Fig. 2 Effect of injection parameter *R* on dimensionless velocity for different non-Newtonian fluids

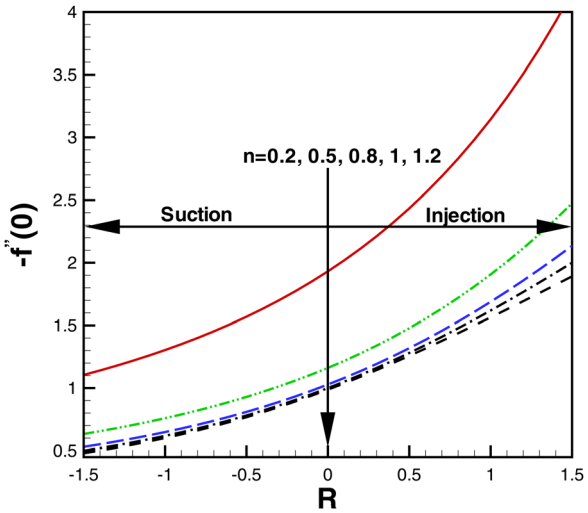

Fig. 3 Variation of dimensionless wall shear stress with suction/injection parameter *R* for different generalized Newtonian fluids

shear stress decreases as the suction parameter increases for each generalized Newtonian fluid, whereas the dimensionless wall shear stress increases with an increase in the injection parameter for each generalized Newtonian fluid. The dimensionless wall shear stress values are found to be highest for pseudoplastic or shear-thinning fluids ($n < 1$), whereas the values are the lowest for dilatant or shear-thickening fluids ($n > 1$). Table 2 shows the dimensionless wall heat transfer rates for each generalized Newtonian fluid (pseudoplastic, Newtonian, and dilatant) for suction and injection cases corresponding to different convective parameters. It is observed that dimensionless wall heat transfer rates approach the constant wall temperature case ($\lambda = 0$ [13]) as $h_c \to \infty$. They increase in the case of injection and decrease in the case of suction.

The effects of suction/injection parameter R on dimensionless velocity are shown in Fig. 2 for different generalized Newtonian fluids. There is no effect of convective and nanofluid parameters on the dimensionless velocity. As expected, the dimensionless velocity is higher in the case of suction. As a result, the velocity boundary layer thickness is larger for the suction case. Due to the shear-thinning effect of power-law fluids, the dimensionless velocity for pseudoplastic fluids is higher than Newtonian fluids, whereas, for the dilatant fluids the dimensionless velocity is lower than the Newtonian fluids. The variation of the dimensionless wall shear stress with suction/injection parameter is illustrated in Fig. 3 for different power-law fluids. It is clear that the dimensionless wall shear stress increases with an increase in suction/injection parameter. The dimensionless wall shear stress is found to be larger for pseudoplastic fluids than dilatant fluids. This is due to the shear thinning effect of the power-law fluids.

The effect of generalized Prandtl numbers, suction/injection, convective, and non-Newtonian nanofluid parameters on dimensionless temperature is depicted in Figs. 4 and 5 for different power-law nanofluids. Figure 4(*a*) shows the effect of injection on dimensionless temperature for different power-law nanofluids. It can be seen that, in case of no injection, the dimensionless temperature is higher for each power-law nanofluid. As the injection parameter increases, the dimensionless temperature decreases for each power-law nanofluid. An increase in the injection parameter also decreases the thickness of the thermal boundary layer. The effect of convective parameter on the dimensionless temperature is illustrated in Fig. 4(*b*) for different power-law fluids. As the convective parameter increases, the dimensionless temperature increases and approaches the isothermal condition. The dimensionless temperature of pseudoplastic fluids is found to be higher than Newtonian and dilatant fluids. The effect of generalized Prandtl numbers on dimensionless temperature for different power-law nanofluids is shown in Fig. 5(*a*). As expected, the thermal boundary layer thickness decreases with an increase in the generalized Prandtl number. The effect of the generalized thermophoresis parameter is to increase the dimensionless temperature which is shown in Fig. 5(*b*) for different power-law nanofluids. The effect of generalized Brownian motion parameter on the

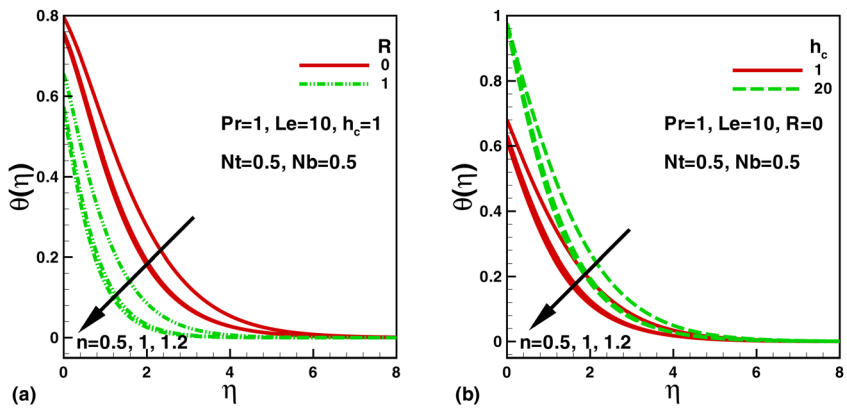

Fig. 4 Effect of injection and convective parameters on dimensionless temperature for different non-Newtonian nanofluids

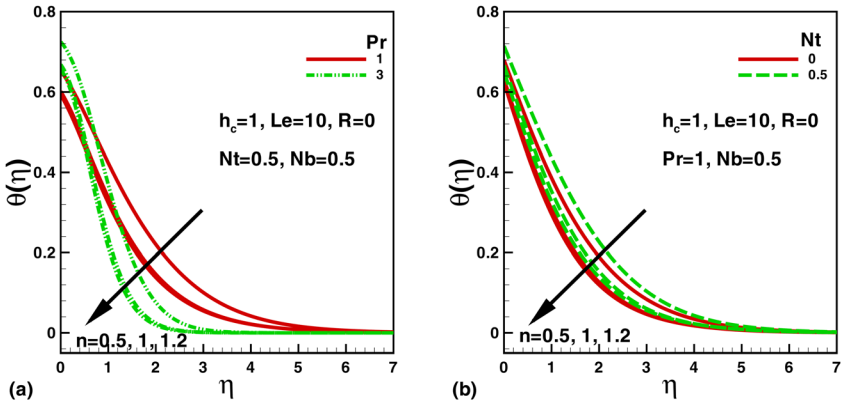

Fig. 5 Effect of generalized Prandtl number Pr and thermophoresis parameter on dimensionless temperature for different non-Newtonian nanofluids

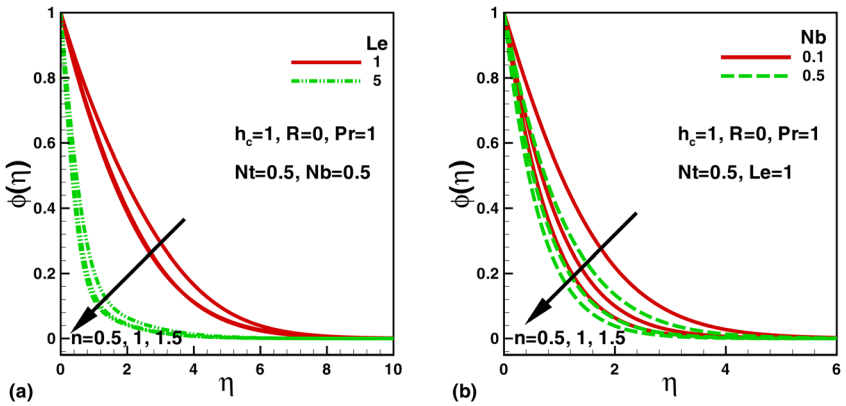

Fig. 6 Effect of generalized Lewis number Le and Brownian motion parameter on dimensionless nanoparticle concentration for different non-Newtonian nanofluids

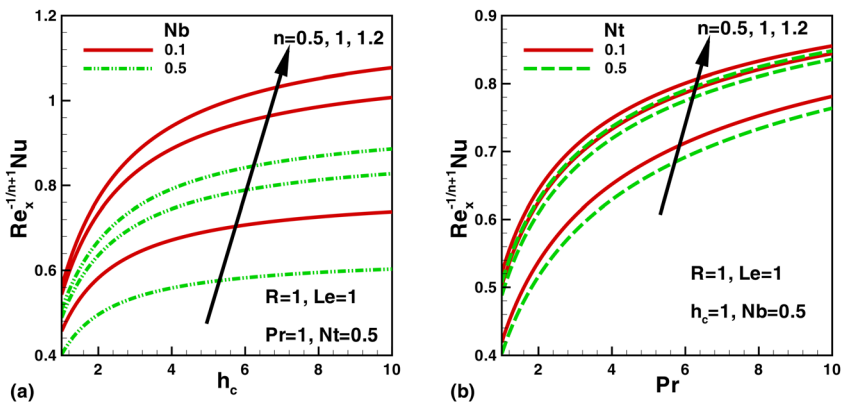

Fig. 7 Variation of dimensionless heat transfer rates with convective parameter and generalized Prandtl number for different power-law nanofluids

dimensionless temperature (not shown here) is found to be the same for different power-law nanofluids. It was observed that the dimensionless temperature increases with an increase in the generalized Brownian motion parameter.

The effects of different parameters on the dimensionless nanoparticle concentration are shown in Figs. 6(*a*) and 6(*b*) for several power-law nanofluids. Figure 6(*a*) illustrates the effects of generalized Lewis numbers on the dimensionless nanoparticle concentration for pseudoplastic, Newtonian, and dilatant fluids. Like generalized Prandtl numbers, an increase in the generalized Lewis numbers decreases the nanoparticle concentration boundary layer thickness. The dimensionless nanoparticle concentration is found to be higher for pseudoplastic fluids than the dilatant fluids. The effect of generalized Brownian motion parameter Nb on dimensionless nanoparticle concentration is shown in Fig. 6(*b*) for different power-law nanofluids. It can be seen that the nanoparticle concentration decreases with an increase in the generalized Brownian motion parameter Nb. The same effect of generalized thermophoresis parameter Nt on the nanoparticle concentration was observed, which is not shown here.

The variation of the local dimensionless heat transfer rates with different parameters is shown in Figs. 7(*a*) and 7(*b*). In the presence of injection, the variation of the local dimensionless heat transfer rates with convective parameter is shown in Fig. 7(*a*) for

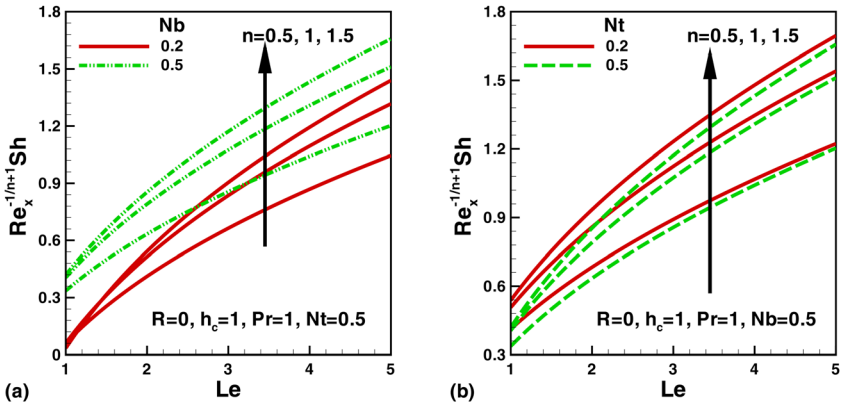

Fig. 8 Variation of dimensionless mass transfer rates with generalized Lewis number, Brownian motion, and thermophoresis parameters for different non-Newtonian nanofluids

three power-law nanofluids with two different values of generalized Brownian motion parameter. It can be seen that the local dimensionless heat transfer rates increase with the convective parameter and approaches the isothermal values as $h_c \to \infty$. It is observed that the local dimensionless heat transfer rates decrease with an increase in the generalized Brownian motion parameter. For dilatant fluids, the local dimensionless heat transfer rates are found to be higher than pseudoplastic fluids for the selected parameters. Figure 7(*b*) shows the variation of the local dimensionless heat transfer rates with the generalized Prandtl numbers for two different values of the generalized thermophoresis parameter. It can be seen that the local dimensionless heat transfer rates increase with the generalized Prandtl numbers. This is only due to a decrease of thermal boundary layer thickness with the generalized Prandtl numbers. The local dimensionless heat transfer rates decrease with an increase in the generalized thermophoresis parameter and increase with an increase in the power-law index. Again, the local dimensionless heat transfer rates are found to be higher for dilatant fluids than pseudoplastic fluids.

The variation of the local dimensionless mass transfer rates with different parameters is shown in Figs. 8(*a*) and 8(*b*) for different power-law nanofluids. Figure 8(*a*) illustrates the variation of the local dimensionless mass transfer rates with generalized Lewis numbers and the generalized Brownian motion parameter for different power-law nanofluids. It is clear from Fig. 8(*a*) that local dimensionless mass transfer rates increase with Le and with the generalized Brownian motion parameter. Like the local dimensionless heat transfer rates, the local dimensionless mass transfer rates are also higher for dilatant fluids than pseudoplastic fluids. The variation of the local dimensionless mass transfer rates with generalized Lewis numbers and thermophoresis parameter is shown in Fig. 8(*b*) for different power-law nanofluids. The local dimensionless mass transfer rates decrease with an increase in *Nt*. It is important to note that the generalized Lewis numbers have strong effects on the local dimensionless mass transfer rates.

4 Conclusions

The work of Hassanien et al. [13] is extended to analyze the behavior of non-Newtonian nanofluids over a stretching surface with convective boundary condition and uniform surface nanoparticle concentration. A similarity solution is obtained that depends on different power-law nanofluid suction/injection, temperature, and nanofluid concentration parameters. The dependency of the skin friction, the local Nusslelt, and the Sherwood numbers on these parameters is investigated numerically. It is found that the

(i) Dimensionless velocity, temperature, and nanofluid concentration are higher for pseudoplastic fluids than dilatant fluids.
(ii) Skin friction is higher for pseudoplastic fluids than dilatant fluids.
(iii) As the convective parameter increases, the dimensionless temperature and the heat transfer rates approaches the isothermal values.
(iv) Local dimensionless heat and mass transfer rates are higher for dilatant fluids than pseudoplastic fluids.

Nomenclature

B = constant
C = nanoparticle volume fraction
C_f = skin friction
C_w = nanoparticle volume fraction at the stretching surface
C_∞ = ambient nanoparticle volume fraction
D_B = Brownian diffusion coefficient
D_T = thermophoretic diffusion coefficient
$f(\eta)$ = dimensionless stream function
$f'(\eta)$ = dimensionless velocity as function of stream function
$f'(0)$ = dimensionless velocity at the surface
h_c = convective parameter
K = thermal conductivity
Le = generalized Lewis number
Nb = generalized Brownian motion parameter
Nt = generalized thermophoresis parameter
Nu_x = local Nusselt number
n = power-law parameter
Pr = generalized Prandtl number
R = suction/injection parameter
Re_x = local generalized Reynolds number
Sh_x = local Sherwood number
T_f = fluid temperature
T_w = temperature at the stretching surface
T_∞ = ambient temperature
u, v = velocity components along x- and y-axes
$u_w(x)$ = velocity of the stretching sheet
x, y = Cartesian coordinates (x-axis is along the stretching surface and y-axis is normal to it)

Greek Symbols

α = thermal diffusivity
η = similarity variable
$\phi(\eta)$ = rescaled nanoparticle volume fraction
λ = temperature parameter
μ = dynamic viscosity of the fluid
ν = kinematic viscosity of the fluid
ρ_f = fluid density
ρ_p = nanoparticle mass density

$(\rho c)_f$ = heat capacity of the fluid
$(\rho c)_p$ = effective heat capacity of the nanoparticle material
ψ = stream function
τ = ratio between the effective heat capacity of the nanoparticle material and heat capacity of the fluid
$\theta(\eta)$ = dimensionless temperature

References

[1] Crane, L. J., 1970, "Flow Past a Stretching Plate," Z. Angew. Math. Phys., **21**, pp. 645–647.
[2] Lakshmisha, K. N., Venkateswaran, S., and Nath, G., 1988, "Three-Dimensional Unsteady Flow With Heat and Mass Transfer Over a Continuous Stretching Surface," ASME J. Heat Transfer, **110**, pp. 590–595.
[3] Wang, C. Y., 1984, "The Three-Dimensional Flow Due to a Stretching Flat Surface," Phys. Fluids, **27**, pp. 1915–1917.
[4] Andersson, H. I., and Dandapat, B. S., 1991, "Flow of a Power-Law Fluid Over a Stretching Sheet," Stability and Applied Analysis of Continuous Media, **1**, pp. 339–347.
[5] Magyari, E., and Keller, B., 2000, "Exact Solutions for Self-Similar Boundary-Layer Flows Induced by Permeable Stretching Walls," Eur. J. Mech. B/Fluids, **19**, pp. 109–122.
[6] Velggaar, J., 1977, "Laminar Boundary Layer Behavior on Continuous Accelerating Surfaces," Chem. Eng. Sci., **32**, pp. 1517–1525.
[7] Wang, C. Y., 1989, "Free Convection on a Vertical Stretching Surface," Z. Angew. Math. Mech., **69**, pp. 418–420.
[8] Tsou, F., Sparrow, E., and Goldstein, R. J., 1967, "Flow and Heat Transfer in the Boundary Layer on a Continuous Moving Surface," Int. J. Heat Mass Transfer, **10**, pp. 219–235.
[9] Gupta, P. S., and Gupta, A. S., 1977, "Heat and Mass Transfer on a Stretching Sheet With Suction or Blowing," Can. J. Chem. Eng., **55**, pp. 744–746.
[10] Grubka, L. J., and Bobba, K. M., 1985, "Heat Transfer Characteristics of a Continuous Stretching Surface With Variable Temperature," ASME J. Heat Transfer, **107**, pp. 248–250.
[11] Hassanien, I. A., and Gorla, R. S. R., 1990, "Heat Transfer to a Micropolar Fluid From a Nonisothermal Stretching Sheet With Suction and Blowing," Acta Mech., **84**, pp. 191–201.
[12] Gorla, R. S. R., and Sidawi, I., 1994, "Free Convection on a Vertical Stretching Surface With Suction and Blowing," Appl. Sci. Res., **52**(3), pp. 247–257.
[13] Hassanien, I. A., Abdullah, A. A., and Gorla, R. S. R., 1998, "Flow and Heat Transfer in a Power-Law Fluid Over a Nonisothermal Stretching Sheet," Math. Comput. Modell., **28**(9), pp. 105–116.
[14] Buongiorno, J., 2006, "Convective Transport in Nanofluids," ASME J. Heat Transfer, **128**, pp. 240–250.
[15] Kuznetsov, A. V., and Nield, D. A., 2010, "Natural Convective Boundary-Layer Flow of a Nanofluid Past a Vertical Plate," Int. J. Thermal Sci., **49**(2), pp. 243–247.
[16] Khan, W. A., and Pop, I., 2010, "Boundary-Layer Flow of a Nanofluid Past a Stretching Sheet," Int. J. Heat Mass Transfer, **53**, pp. 2477–2483.
[17] Vajravelu, K., Prasad, K. V., Lee, J., Lee, C., Pop, I., and Van Gorder, R. A., 2011, "Convective Heat Transfer in the Flow of Viscous Ag–Water and Cu–Water Nanofluids Over a Stretching Surface," Int. J. Thermal Sci., **50**(5), pp. 843–851.
[18] Makinde, O. D., and Aziz, A., 2011, "Boundary Layer Flow of a Nanofluid Past a Stretching Sheet With a Convective Boundary Condition," Int. J. Thermal Sci., **50**(7), pp. 1326-1332.
[19] Chen, H., Yang, W., He, Y., Ding, Y., Zhang, L., Tan, C., Lapkin, A. A., and Bavykin, D. V., 2008, "Heat Transfer and Flow Behavior of Aqueous Suspensions of Titanate Nanotubes (Nanofluids)," Powder Technol., **183**(1), pp. 63–72.
[20] Ding, Y., Chen, H., He, Y., Lapkin, A., Yeganeh, M., Siller, L., and Butenko, Y. V., 2007, "Forced Convective Heat Transfer of Nanofluids," Adv. Powder Technol., **18**(6), pp. 813–824.
[21] Ding, Y., Chen, H., Musina, Z., Jin, Y., Zhang, T., Witharana, S., and Yang, W., 2010, "Relationship Between the Thermal Conductivity and Shear Viscosity of Nanofluids," Phys. Scr., **T139**, p. 014078.
[22] Chen, H., Ding, Y., and Tan, C., 2007, "Rheological Behaviour of Nanofluids," New J. Phys., **9**(10), p. 367.
[23] He, Y., Men, Y., Liu, X., Lu, H., Chen, H., and Ding, Y., 2009, "Study on Forced Convective Heat Transfer of Non-Newtonian Nanofluids," Int. J. Thermal Sci., **18**(1), pp. 20–26.